TLR3-Mediated CD8+ Dendritic Cell Activation Is Coupled with Establishment of a Cell-Intrinsic Antiviral State

Szeles, Lajos; Meissner, Felix; Dunand-Sauthier, Isabelle; Thelemann, Christoph; Hersch, Micha; Singovski, Simon; Haller, Sergio; Gobet, Florian; Fuertes Marraco, Silvia A; Mann, Matthias; Garcin, Dominique; Acha-Orbea, Hans; Reith, Walter

How to cite

SZELES, Lajos et al. TLR3-Mediated CD8+ Dendritic Cell Activation Is Coupled with Establishment of a Cell-Intrinsic Antiviral State. In: The Journal of immunology, 2015, vol. 195, n° 3, p. 1025–1033. doi: 10.4049/jimmunol.1402033

This publication URL: https://archive-ouverte.unige.ch//unige:79564

Publication DOI: 10.4049/jimmunol.1402033

The Journal of Immunology

TLR3-Mediated CD8$^+$ Dendritic Cell Activation Is Coupled with Establishment of a Cell-Intrinsic Antiviral State

Lajos Széles, Felix Meissner, Isabelle Dunand-Sauthier, Christoph Thelemann, Micha Hersch, Simon Singovski, Sergio Haller, Florian Gobet, Silvia A. Fuertes Marraco, Matthias Mann, Dominique Garcin, Hans Acha-Orbea and Walter Reith

J Immunol 2015; 195:1025-1033; Prepublished online 22 June 2015;
doi: 10.4049/jimmunol.1402033
http://www.jimmunol.org/content/195/3/1025

The Journal of Immunology is published twice each month by
The American Association of Immunologists, Inc.,
9650 Rockville Pike, Bethesda, MD 20814-3994.

Print ISSN: 0022-1767 Online ISSN: 1550-6606.

TLR3-Mediated CD8$^+$ Dendritic Cell Activation Is Coupled with Establishment of a Cell-Intrinsic Antiviral State

Lajos Széles,* Felix Meissner,† Isabelle Dunand-Sauthier,* Christoph Thelemann,‡ Micha Hersch,§ Simon Singovski,* Sergio Haller,‡ Florian Gobet,* Silvia A. Fuertes Marraco,‡,1 Matthias Mann,† Dominique Garcin,¶ Hans Acha-Orbea,‡,2 and Walter Reith*,2

Because of their unique capacity to cross-present Ags to CD8$^+$ T cells, mouse lymphoid tissue–resident CD8$^+$ dendritic cells (DCs) and their migratory counterparts are critical for priming antiviral T cell responses. High expression of the dsRNA sensor TLR3 is a distinctive feature of these cross-presenting DC subsets. TLR3 engagement in CD8$^+$ DCs promotes cross-presentation and the acquisition of effector functions required for driving antiviral T cell responses. In this study, we performed a comprehensive analysis of the TLR3-induced antiviral program and cell-autonomous immunity in CD8$^+$ DC lines and primary CD8$^+$ DCs. We found that TLR3-ligand polyinosinic-polycytidylic acid and human rhinovirus infection induced a potent antiviral protection against Sendai and vesicular stomatitis virus in a TLR3 and type I IFN receptor–dependent manner. Polyinosinic-polycytidylic acid–induced antiviral genes were identified by mass spectrometry–based proteomics and transcriptomics in the CD8$^+$ DC line. Nanostring nCounter experiments confirmed that these antiviral genes were induced by TLR3 engagement in primary CD8$^+$ DCs, and indicated that many are secondary TLR3-response genes requiring autocrine IFN-β stimulation. TLR3-activation thus establishes a type I IFN–dependent antiviral program in a DC subtype playing crucial roles in priming adaptive antiviral immune responses. This mechanism is likely to shield the priming of antiviral responses against inhibition or abrogation by the viral infection. It could be particularly relevant for viruses detected mainly by TLR3, which may not trigger type I IFN production by DCs that lack TLR3, such as plasmacytoid DCs or CD8$^-$ DCs. *The Journal of Immunology*, **2015, 195: 1025–1033.**

Dendritic cells (DCs) comprise distinct subtypes differing in their phenotype, function, localization, and migratory properties (1–4). Four main cell types are generally categorized as DCs: plasmacytoid DCs (pDCs), Langerhans cells, monocyte-derived DCs (MoDCs), and classical or conventional DCs (cDCs) (1, 4). Major mouse cDC subtypes include CD8$^+$ and CD8$^-$ DCs in lymphoid tissues, and CD103$^+$ and CD11b$^+$ DCs in nonlymphoid organs (1, 5).

CD8$^+$ DCs, and the functionally and developmentally related CD103$^+$ DCs, are specialized for inducing antiviral cytotoxic CTL responses because they are particularly efficient at cross-presenting peptides derived from exogenous Ags in the context of MHC class I molecules (1, 6–9). Ags derived from infected tissues are believed to be transferred to CD8$^+$ DCs by lymphatic drainage or migratory DCs (3). Activated CD8$^+$ DCs secrete cytokines, such as IL-12, IL-6, and type I and III IFNs, promoting immune responses against viruses and parasitic protozoans (10–12).

DCs induce appropriately tailored immune responses by detecting, integrating, and responding to pathogen-associated molecular patterns and host-derived signals, including danger-associate molecular patterns and cytokines. Signaling through the receptors of these signals triggers and/or promotes the maturation (activation) of DCs (3). In addition to their key effects on maturation, these signals can modify other features of DCs. For example, CD103$^+$ DCs can acquire protection against viral infection in vivo via type I IFNs (I-IFN) (13, 14). Pathogen-associated molecular patterns are detected by pattern recognition receptors, including transmembrane TLRs, intracellular receptors, such as RIG-I–like receptors, and NOD-like receptors (15, 16).

Mouse CD8$^+$ and CD103$^+$ DCs express the highest levels of TLR3 (5, 15), a dsRNA receptor that detects viral genomes or replication intermediates in endolysosomal compartments (17). TLR3 signals via the adaptor protein TRIF and activates signal-regulated transcription factors, of which the best characterized are NF-κB, AP-1, and IRF3 (16, 18). Studies with mouse bone marrow–derived DCs (BMDCs) have shown that TLR-induced regulatory programs also involve numerous other transcription factors and

*Department of Pathology and Immunology, Faculty of Medicine, University of Geneva, CH-1211 Geneva, Switzerland; †Proteomics and Signal Transduction, Max Planck Institute of Biochemistry, D-82152 Martinsried, Germany; ‡Department of Biochemistry, University of Lausanne, CH-1066 Epalinges, Switzerland; §Computational Biology Group, Department of Medical Genetics, University of Lausanne, CH-1005 Lausanne, Switzerland; and ¶Department of Microbiology and Molecular Medicine, Faculty of Medicine, University of Geneva, CH-1211 Geneva, Switzerland

[1]Current address: Ludwig Cancer Center, University of Lausanne, Épalinges, Switzerland.

[2]H.A.-O. and W.R. contributed equally to this work.

Received for publication August 7, 2014. Accepted for publication May 20, 2015.

This work was supported by Swiss National Science Foundation Grant CRSI33_130444 to H.A.-O., W.R., and M.M.

The microarray data presented in this article have been submitted to the Gene Expression Omnibus (http://www.ncbi.nlm.nih.gov/geo/) under accession number GSE57512.

Address correspondence and reprint requests to Prof. Walter Reith, Department of Pathology and Immunology, Faculty of Medicine, University of Geneva, Rue Michel-Servet 1, CH-1211 Geneva, Switzerland. E-mail address: Walter.Reith@unige.ch

The online version of this article contains supplemental material.

Abbreviations used in this article: 7AAD, 7-aminoactinomycin D; BMDC, bone marrow–derived DC; cDC, conventional DC; CHX, cycloheximide; DC, dendritic cell; HRV, human rhinovirus; I-IFN, type I IFN; III-IFN, type III IFN; ImmGen, Immunological Genome Project; ISG, IFN-stimulated gene; MoDC, monocyte-derived DC; MS, mass spectrometry; pDC, plasmacytoid DC; pIC, polyinosinic-polycytidylic acid; qPCR, real time quantitative RT-PCR; SeV, Sendai virus; SeV-RFP, SeV expressing red fluorescent protein; VSV, vesicular stomatitis virus; WT, wild-type.

coregulators controlling complex transcriptional responses (19, 20). Activation of cDCs by viral dsRNA or synthetic dsRNA-analogs, such as polyinosinic-polycytidylic acid (pIC), triggers maturation, promotes cross-priming, confers antiviral protection, and induces production of I-IFN and type III IFNs (III-IFNs), chemokines (such as CXCL10 and CCL5), and inflammatory cytokines (such as IL-6 and TNF-α) (10, 11, 18, 21, 22).

TLR3-activated antiviral genes can be induced by two mechanisms, directly and indirectly via I-IFN production (23). Certain IFN-stimulated genes (ISGs) can interfere with diverse steps in viral infections, including viral entry, uncoating, replication, assembly, budding, and release (24, 25). TLR3 agonist-induced expression of I-IFN and antiviral effectors has been implicated in the establishment of a cell-autonomous antiviral state in diverse cell types, such as fibroblasts, hepatocytes, mouse bone marrow–derived macrophages, BMDCs, and human MoDCs (21, 23, 26–30), although in many studies the involvement of TLR3 was not demonstrated and/or that of intracellular dsRNA sensors was not excluded.

Despite the pivotal role of CD8$^+$ DCs in driving antiviral immunity (31) and their distinctive property of high TLR3 expression (5, 15, 32) the TLR3-induced antiviral programs have not been characterized in CD8$^+$ DCs. To investigate these processes, we performed functional experiments combined with large-scale transcriptomic and proteomic analyses with CD8$^+$ DC lines retaining all distinctive features of their in vivo counterparts (see Ref. 33 and *Results*). Key findings were verified in primary CD8$^+$ DCs. The results demonstrate that TLR3 engagement in CD8$^+$ DCs activates a cell-autonomous antiviral program requiring amplification by a positive feedback loop mediated by autocrine I-IFN stimulation.

Materials and Methods

Cells

Wild-type (WT) (MuTu1940), *Tlr3*$^{-/-}$, and *Ifnar1*$^{-/-}$ CD8$^+$ DC lines were established and cultured as described previously (33, 34). Splenic CD8$^+$ DCs were isolated from Flt3L-transgenic mice (35) or WT C57BL/6J mice using CD8$^+$ DC purification kit (130-091-169; Miltenyi Biotec). DCs were stimulated with 5 μg/ml pIC [poly(I:C) HMW, tlrl-pic; Invivogen], 10^3 U/ml IFN-β (12401-1; PBL Laboratories), 10^4 U/ml IFN-α (130-093-131; Miltenyi Biotec), 10 ng/ml IFN-γ (34-8311-85; eBioscience), 100 ng/ml IFNλ3 (12820-1; PBL Laboratories), and 100 ng/ml LPS (ALX-581-009; Alexis-Enzo). The following Abs were used to detect DC and maturation markers: anti-CD80 (16-10A1; BD Biosciences), anti-CD8a (53-6.7; eBioscience), and anti-CD11c (N418; eBioscience). Dependence of pIC-induced expression on de novo protein synthesis was assessed by pretreatment for 0.5 h with 20 μg/ml cycloheximide (CHX; Sigma-Aldrich). Animal husbandry and isolation of splenic CD8$^+$ DCs from Flt3L-transgenic mice were approved by and performed in accordance with guidelines from the Animal Research Committee of the University of Lausanne and University of Geneva.

Viral infections

Sendai virus (SeV)-RFP (tdTomato) and SeV-GFP were generated by D.G. (36). Vesicular stomatitis virus (VSV) and a clinical human rhinovirus (HRV) strain (HRV14) were gifts from J. Perrault and C. Tapparel. RFP (tdTomato) or GFP expression in infected cells was assessed by flow cytometry or microscopy. Cell viability was assessed by phase-contrast microscopy or flow cytometry using 7-aminoactinomycin D (7AAD) staining.

Infection of the DC cell line. SeV expressing red fluorescent protein (SeV-RFP)– or VSV-infected cells were not pretreated, pretreated for 18 h with 5 μg/ml pIC or I-IFNs (10^3 U/ml IFN-β or 10^4 U/ml IFN-α), or preinfected for 18 h with HRV. Uninfected cells were used as negative controls. The capacity of pIC to induce an antiviral state was also tested by adding it at various time points ranging from 18 h before to 16 h post SeV-RFP infection. The antiviral state was induced most efficiently when pIC was added between 6 and 18 h before infection. pIC was less efficient or ineffective when added together with or after SeV infection. Infection frequencies were determined 24 h postinfection by quantifying RFP positivity.

Infection of primary CD8$^+$ DCs. Splenic CD8$^+$ DCs were pre-enriched by negative selection using a CD8$^+$ DC purification kit (130-091-169; Miltenyi Biotec). Further purification by positive selection with anti-CD8a Ab was avoided because it reduced infection efficiency, probably by triggering spontaneous maturation. For experiments involving ex vivo pretreatment (6 h) with pIC (5 μg/ml) or IFN-β (10^3 U/ml), cells were isolated from untreated C57BL/6J WT mice. For assessing the effect of in vivo pIC treatment, cells were isolated 20 h after i.p. injection of C57BL/6J WT mice with PBS or 50 μg pIC. Cells were infected ex vivo by SeV-GFP. Higher multiplicities of infection were required for primary CD8$^+$ DCs (50 PFU/cell) compared with the DC line (1 PFU/cell) to achieve efficient infection. Infection frequencies were determined 16 h postinfection by quantifying GFP positivity of CD8$^+$CD11c$^+$CD80$^+$ DCs. Similar results, with lower infection frequencies, were obtained by gating on CD8$^+$CD11c$^+$ cells.

ELISA

IFN-β was quantified in supernatants by ELISA using an IFN-β kit (PBL Assay Science) according to the manufacturer's instructions.

Real time quantitative RT-PCR

RNA was isolated using peqGOLD TriFast reagent (PEQLAB). Real time quantitative RT-PCR (qPCR) was performed using the SuperScript II First-Strand Synthesis System (Invitrogen), iQ SYBR Green Supermix, and the iCycler iQ Real-Time PCR Detection System (Bio-Rad). The comparative cycle threshold method was used to calculate expression relative to Rplp0. Primer sequences are supplied in Supplemental Table I.

Transcriptomics

Total RNA was isolated using RNeasy kits (Qiagen). Processing, labeling, hybridization to Affymetrix GeneChip Mouse 1.0 ST Arrays, and scanning were conducted at the Genomics Platform (University of Geneva) according to the manufacturer's instructions. Cel image files were imported to GeneSpring 12.6.1 software. Normalization was performed using robust multiarray average summarization algorithm. Significantly regulated genes were identified using a 2-fold cutoff and moderated *t* test with the Benjamini-Hochberg procedure for multiple test correction (adjusted $p < 0.05$). Microarray data were deposited in Gene Expression Omnibus (http://www.ncbi.nlm.nih.gov/geo/) under accession number GSE57512.

Liquid chromatography–mass spectrometry–based quantitative proteomics

Cells were lysed in 2% SDS, Tris HCl pH 7.6. Proteins were denatured by boiling and sonication in the presence of dithiothreitol. Cysteine reduction was followed by alkylation with iodoacetamide. Proteins were precipitated with 80% acetone for 16 h, resolubilized in 6 M urea/2 M thiourea, digested for 3 h with 1 μg LysC/50 μg protein (Wako), diluted 1:4, and digested for 16 h at room temperature with 1 μg trypsin/50 μg protein (Promega). Peptides were desalted on reversed-phase C18 material and eluted with 80% acetonitrile in 0.5% acetic acid. The volume was reduced in a SpeedVac and peptides were acidified with 2% acetonitrile, 0.1% trifluoroacetic acid in 0.1% formic acid.

A nanoflow UHPLC instrument (Easy nLC; Thermo Fisher Scientific) was coupled online to a Q Exactive mass spectrometer (Thermo Fisher Scientific) with a nanoelectrospray ion source (Thermo Fisher Scientific). Chromatography columns were packed with ReproSil-Pur C18-AQ 1.8 μm resin (Dr. Maisch GmbH). Two-microgram peptides were separated with a gradient of 5–60% buffer B (80% acetonitrile in 0.1% formic acid) at a flow rate of 200 nl/min over 240 min using 50-cm analytical columns. Mass spectrometry (MS) data were acquired with a data-dependent Top10 acquisition method dynamically choosing the most abundant precursor ions from the survey scan (300–1650 Th) for higher-energy collisional dissociation fragmentation. Survey scans were acquired at a resolution of 70,000 at m/z 200. Unassigned precursor ion charge states as well as singly charged species were rejected. The isolation window was set to 2 Th and normalized collision energies to 25. The maximum ion injection times for the MS1 scan and the MS2 scans were 20 and 60 ms with ion target values of 3E6 and 1e6, respectively. Selected sequenced ions were dynamically excluded for 40 s. Data were acquired using Xcalibur software.

Mass spectra were analyzed with MaxQuant software version 1.2.6.20 using the Andromeda search engine. The allowed mass deviation was set to 6 ppm for monoisotopic precursor ions and 0.5 Da for MS/MS peaks. Enzyme specificity was set to trypsin, defined as C-terminal to arginine and

lysine including proline, and a maximum of three missed cleavages were allowed. Carbamidomethylcysteine was set as a fixed modification, N-terminal acetylation and methionine oxidation as variable modifications. The data were searched against the mouse Uniprot sequence database (Uniprot version 2012-02-25) supplemented with frequently observed contaminants and concatenated with the reversed versions of all sequences. The required false-positive rate was set to 1% at the peptide and 1% at the protein level, and the minimum required peptide length was set to 7 aa. Protein identification required at least one unique or razor peptide per protein group. Quantification in MaxQuant was performed using label-free quantification algorithm with fast label-free quantification and match between runs enabled. A peptide library derived by digestion of lysates from MuTu cells activated through different cellular receptors was used for matching.

Contaminants, reverse identification, and proteins only identified by site were excluded from further data analysis. Missing values were imputed by random sampling from a generated narrow normal distribution around the detection limit for proteins. Imputed data were imported to GeneSpring 12.6.1 software. Normalization was performed using robust multiarray average summarization algorithm. Significantly upregulated proteins were identified using a 2-fold cutoff and moderated t test with the Benjamini-Hochberg procedure for multiple test correction (adjusted $p < 0.05$).

Nanostring nCounter analysis

CodeSets for Nanostring nCounter analysis (37) were constructed for housekeeping (control) genes, and for genes encoding antiviral ISGs, cytokines, and maturation markers. Total RNA was purified using peqGOLD TriFast reagent (PEQLAB). A total of 100 ng RNA was hybridized with the CodeSets and loaded into the nCounter prep station, followed by quantification using the nCounter Digital Analyzer at the Genomics Platform (University of Geneva).

Results

CD8$^+$ DC line represents a reliable model for primary CD8$^+$ DCs

We previously reported that our mouse CD8$^+$ DC lines retained all major phenotypic and functional features of their in vivo counterparts, including characteristic cell-surface marker expression, responsiveness to TLR stimuli, patterns of cytokine and chemokine production, cross-presentation capacity, and T cell–stimulatory properties (33). This was further confirmed by studying the expression of 257 genes identified as cDCs, pDCs, CD8$^-$ DCs, CD8$^+$ DCs, and CD103$^+$ signature genes by the Immunological Genome Project (ImmGen) (5). Expression of these genes was remarkably similar between the CD8$^+$ DC line, CD8$^+$ DCs, and tissue CD103$^+$ DCs (Supplemental Fig. 1). In principal component analysis, the CD8$^+$ DC line clustered with these primary DC subsets (Fig. 1A). Genes encoding nucleic acid–sensing TLRs (*Tlr3*, *Tlr7*, *Tlr9* and *Tlr13*) were also expressed similarly between the CD8$^+$ DC line, CD8$^+$ DCs, and CD103$^+$ DCs (Fig. 1B). *Tlr3* was notably expressed strongly in the CD8$^+$ DC line (5) (Supplemental Fig. 1). Finally, Nanostring nCounter analyses indicated that selected genes were induced comparably by pIC in the CD8$^+$ DC line and splenic CD8$^+$ DCs (Fig. 1C).

TLR3-dependent induction of an antiviral state in CD8$^+$ DCs

Establishment of a pIC-induced antiviral state in the CD8$^+$ DC line was examined by assessing protection against SeV and VSV (Fig. 2). Such negative ssRNA viruses are not detected by TLR3 because their replication does not produce detectable amounts of dsRNA (38). They consequently do not induce maturation of CD8$^+$ DCs, which express low levels of cytoplasmic RIG-I–like receptors, the major sensors for negative ssRNA viruses in cDCs (32). An assay based on infection with SeV-RFP was used (Fig. 2A). Examination of CD80 expression confirmed that SeV-RFP did not induce maturation of the CD8$^+$ DC line (Fig. 2B). Quantification of RFP demonstrated that pretreatment of the CD8$^+$ DC line with pIC blocked SeV-RFP replication similarly to IFN-α

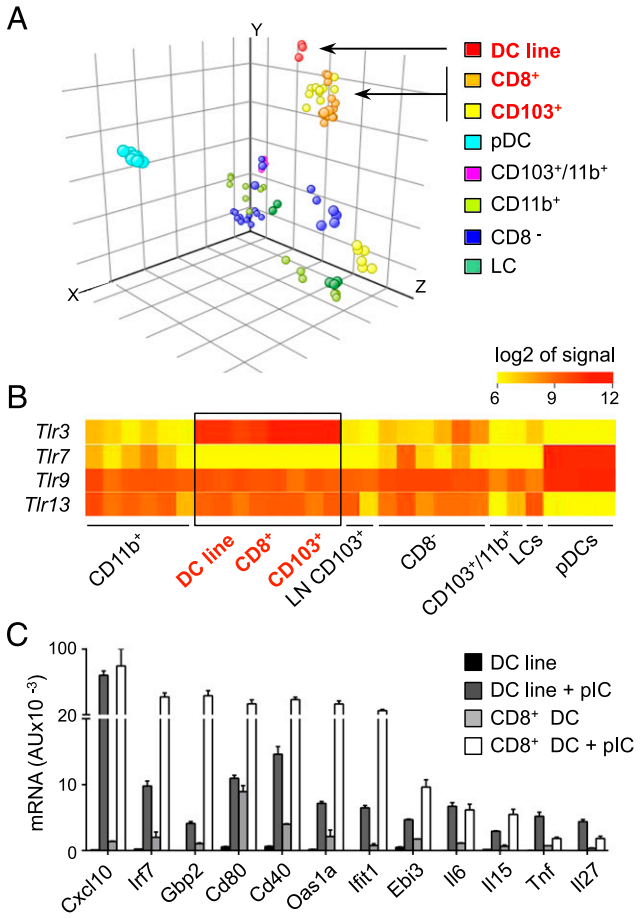

FIGURE 1. TLR3 is expressed selectively in CD8$^+$ and CD103$^+$ DCs. (**A**) Principal component analysis was performed to compare the CD8$^+$ DC line with primary DC subsets using ImmGen microarray data for 257 differentially expressed signature genes. Our microarray data were used for the CD8$^+$ DC line. The CD8$^+$ DC line (red dots, three measurements) clusters with lymph node–resident CD8$^+$ (orange) and tissue-resident CD103$^+$ (yellow) DCs. Notably, other CD103$^+$ DCs isolated from lymphoid tissues cluster separately. (**B**) *Tlr3*, *Tlr7*, Tlr9, and *Tlr13* expression is compared between the CD8$^+$ DC line and the indicated DC subsets. (**C**) mRNA expression for the indicated genes was quantified by Nanostring nCounter in the CD8$^+$ DC line and splenic CD8$^+$ DCs treated for 0 and 6 h with pIC. Data expressed in arbitrary units (AU) were normalized relative to *Eef1a1*, *Ppia*, *Rpl13a*, *Rplp0*, and *Sdha*. The mean and SD derived from three independent experiments are shown.

(Fig. 2C, 2E). For VSV, which is highly cytopathic, cell viability was evaluated by 7AAD staining. Pretreatment of the CD8$^+$ DC line with pIC abrogated the cytopathic effect of VSV to the same extent as IFN-α (Fig. 2D). Examination of cell morphology confirmed that VSV-induced cell death was inhibited by pIC or IFN-α pretreatment (Fig. 2D). We stimulated the DC line with pIC at various time points (between −18 h and +16 h) relative to infection with SeV-RFP. The most efficient time frame for establishing the antiviral state by pIC was between 6 and 18 h of pretreatment. pIC was less efficient or ineffective when it was administrated together with or after SeV infection (Supplemental Fig. 2B). We next tested whether a viral infection accompanied by the production of dsRNA can induce an antiviral state in the CD8$^+$ DC line. The replication of positive ssRNA viruses proceeds via dsRNA intermediates constituting natural TLR3 ligands (11, 17, 38). As observed for pIC and IFN-α pretreatment, infection of the CD8$^+$ DC line with HRV induced an antiviral state that impaired SeV-RFP replication (Fig. 2E). This correlated with the induction

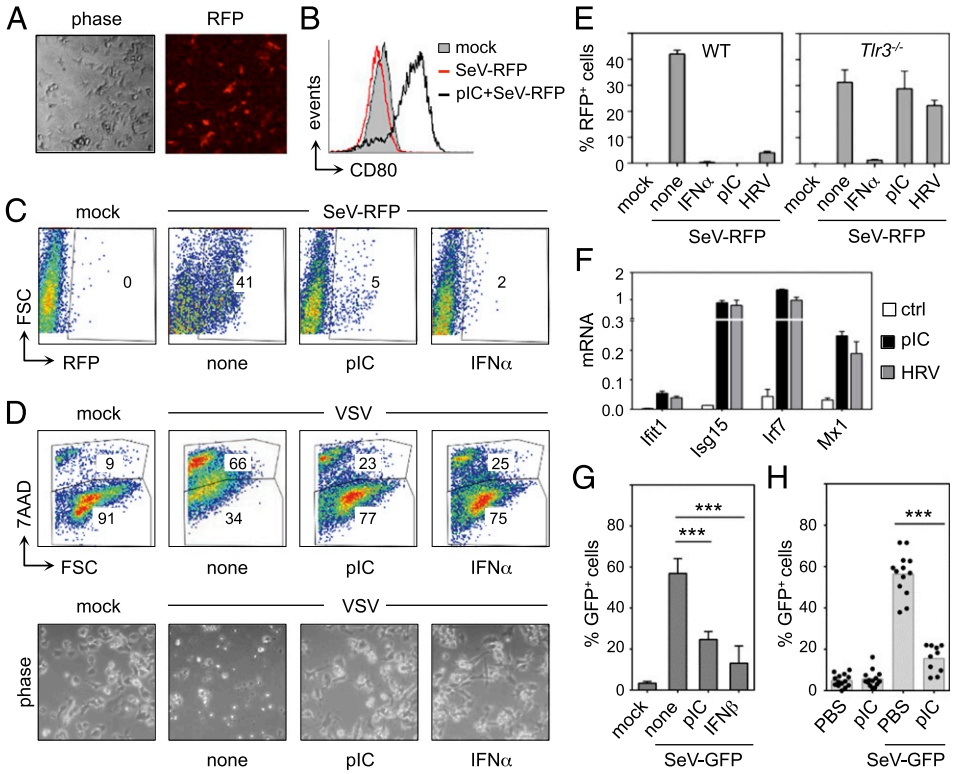

FIGURE 2. Establishment of a TLR3-dependent antiviral state in CD8+ DCs. (**A**) Phase-contrast and fluorescence microscopy images of the CD8+ DC line infected with SeV-RFP. Original magnification ×20. (**B**) Maturation of the CD8+ DC line as assessed by analyzing CD80 expression by flow cytometry. (**C**) RFP+ cells were quantified by flow cytometry 24 h after SeV-RFP infection. (**D**) Cell viability was assessed by 7AAD staining (*top panels*) or phase-contrast microscopy (*bottom panels*, original magnification ×20) after VSV infection of the CD8+ DC line for 16 or 40 h, respectively. (**E**) RFP+ cells were quantified after 24-h SeV-RFP infection of WT and $Tlr3^{-/-}$ CD8+ DC lines. (**F**) *Ifit1*, *Isg15*, *Irf7*, and *Mx1* mRNAs were quantified by qPCR in the CD8+ DC line after 18 h of pIC-stimulation or HRV infection. Expression was normalized relative to *Rplp0*. (B–E) Uninfected cells (mock) were used as negative controls. SeV-RFP– (B, C, and E) or VSV-infected (D) cells were not pretreated (none), pretreated for 18 h with pIC or IFN-α (B–E), or preinfected for 18 h with HRV (E). (E and F) The mean and SD derived from three independent experiments are shown. (B–D) Results are representative of three experiments. (**G**) Splenic CD8+ DCs isolated from WT mice were stimulated for 6 h with IFN-β or pIC, and infected for 16 h with SeV-GFP. Noninfected cells (mock) and untreated cells (none) were used as controls. Infection was quantified by flow-cytometry analysis of GFP. Results show the mean and SD derived from four independent experiments. (**H**) Mice were injected i.p. with 50 μg pIC or PBS 20 h before isolation of splenic CD8+ DCs. The cells were then infected with SeV-GFP for 16 h. Uninfected cells were used as controls. Data points represent individual mice (at least 10 mice/group). Bars indicate the means. $***p < 0.001$.

of primary (*Ifit1*, *Isg15*) and secondary (*Irf7*, *Mx1*) TLR3-response genes (23) (Fig. 2F).

A *Tlr3*-deficient CD8+ DC line was used to determine whether induction of the antiviral state requires TLR3 engagement. Both pIC pretreatment and HRV infection failed to inhibit SeV-RFP replication in $Tlr3^{-/-}$ CD8+ DC cells, whereas the antiviral state was readily conferred by IFN-α (Fig. 2E).

Two approaches were used to evaluate the establishment of a pIC-induced antiviral state in primary CD8+ DCs. First, splenic CD8+ DCs isolated from WT mice were pretreated in vitro with pIC before infection with SeV-GFP (Fig. 2G). Second, SeV-GFP infections were performed with splenic CD8+ DCs isolated from WT mice that had been pretreated with pIC in vivo (Fig. 2H). In both experimental setups, pIC significantly reduced the percentage of infected GFP+ CD8+ DCs. These results indicated that pIC can induce cell-intrinsic antiviral protection in both the CD8+ DC cell line and primary splenic CD8+ DCs.

I-IFNs play a crucial role in establishment of the antiviral state in CD8+ DCs

pIC can induce I-IFN and III-IFN production by CD8+ DCs (10, 11, 22, 39). Neutralizing Abs against I-IFN can inhibit the establishment of a pIC-induced antiviral state in human MoDCs (28). In mouse bone marrow–derived macrophages, some antiviral ISGs such as *Irf7* and *Mx1* are induced indirectly by TLR4 or TLR3 ligands via autocrine I-IFN stimulation (23). These findings prompted us to study the role of IFN signaling in establishment of the TLR3-induced antiviral state in CD8+ DCs. We exploited a CD8+ DC line lacking the gene (*Ifnar1*) encoding a subunit of the I-IFN receptor. pIC- and I-IFN–induced *Irf7* and *Mx1* expression was abolished in $Ifnar1^{-/-}$ cells (Fig. 3A). Conversely, pIC-induced expression of other TLR3-response genes, such as *Ccl5*, *Cd40*, and *Ebi3*, was not affected in $Ifnar1^{-/-}$ cells (data not shown). As expected, IFN-α stimulation could not abrogate SeV-RFP replication in the $Ifnar1^{-/-}$ cells (Fig. 3B). pIC and HRV likewise failed to inhibit SeV-RFP replication in $Ifnar1^{-/-}$ cells, demonstrating that I-IFN is a key mediator of the TLR3-induced antiviral state (Fig. 3B).

We next examined the expression of IFNs and their receptors in CD8+ DCs to evaluate their contributions to induction of the antiviral state. *Ifnb1*, *Ifnl2* (also known as *Il28a*), and *Ifnl3* (also known as *Il28b*) mRNAs were induced in the CD8+ DC line within 2 h after pIC stimulation (Fig. 3C). IFN-β secretion was also induced by pIC and exposure to HRV-infected apoptotic cells, but not by LPS, for which the cognate pattern recognition receptor (TLR4) is not expressed by CD8+ DCs (Fig. 3D). Genes encoding subunits of the I-IFN (*Ifnar1*, *Ifnar2*) and II-IFN (*Ifngr1*, *Ifngr2*) receptors were expressed in the CD8+ DC line. In contrast, of the

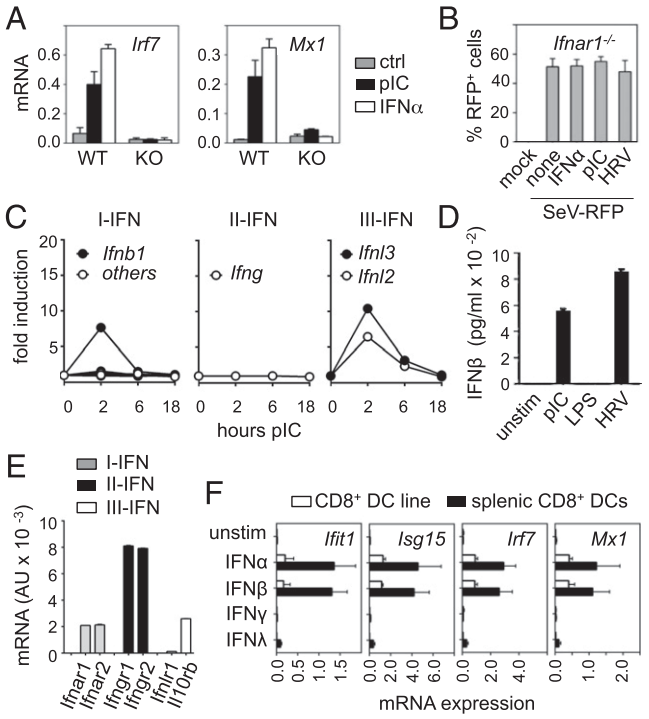

FIGURE 3. IFN dependence of the pIC-induced antiviral state in CD8$^+$ DCs. (**A**) *Irf7* and *Mx1* mRNAs were quantified by qPCR in WT or *Ifnar1* knockout (KO) CD8$^+$ DC lines stimulated for 0 (ctrl) or 6 h with pIC or IFN-α. Expression was normalized relative to *Rplp0*. (**B**) RFP$^+$ cells were quantified in the *Ifnar1*$^{-/-}$ CD8$^+$ DC line after 24 h of SeV-RFP infection. Uninfected cells (mock) were used as negative controls. Cells were left untreated (none), pretreated for 18 h with pIC or IFN-α, or preinfected for 18 h with HRV. (**C**) I-IFN, II-IFN, and III-IFN mRNAs were quantified (microarray analysis) in the CD8$^+$ DC line stimulated for 0, 2, 6, or 18 h with pIC. Others: *Ifna1, 2, 4, 5, 6, 7, 9, 11, 12, 13*, *Ifne*, *Ifnk*, and *Ifnz*. (**D**) IFN-β production was measured by ELISA in culture medium of the CD8$^+$ DC line exposed to pIC, LPS, or HRV-infected HeLa cells. HRV-infected cells were cocultured for 24 h at a 1:3 ratio with the CD8$^+$ DCs. (**E**) mRNAs for genes encoding I-IFN (*Ifnar1*, *Ifnar2*), II-IFN (*Ifngr1*, *Ifngr2*), and III-IFN (*Ifnlr1, Il10rb*) receptor subunits were quantified (microarray analysis) in the CD8$^+$ DC line. (**F**) *Ifit1*, *Isg15*, *Irf7*, and *Mx1* mRNAs were quantified by qPCR in the CD8$^+$ DC line and splenic CD8$^+$ DCs stimulated for 6 h with IFN-α, IFN-β, IFN-γ, or IFN-λ. Expression was normalized relative to *Rplp0*. (A–F) Results are derived from three independent experiments or biological repeats.

genes encoding the III-IFN receptor subunits (*Ifnlr1* and *Il10rb*), only *Il10rb* was expressed (Fig. 3E). Analysis of ImmGen microarray data indicated that primary CD8$^+$ DCs exhibit similar patterns of IFNR subunit expression, including low *Ifnlr1* expression (Supplemental Fig. 2A). In accordance with the pattern of IFNR expression in CD8$^+$ DCs, and known cytokine signaling pathways, *Ifit1*, *Isg15*, *Irf7*, and *Mx1* were induced in the CD8$^+$ DC line and splenic CD8$^+$ DCs by I-IFNs (IFN-α and IFN-β), but not IFN-γ or IFN-λ3 (Fig. 3F). These results indicate that only I-IFN contributes to establishment of the pIC-induced antiviral state in CD8$^+$ DCs, although they produce both IFN-β and III-IFNs.

Identification of pIC-induced antiviral genes in CD8$^+$ DCs

To investigate pIC-induced antiviral genes in CD8$^+$ DCs, we analyzed the transcriptome and proteome of the CD8$^+$ DC line stimulated for various times with pIC, by means of DNA microarray experiments and quantitative MS, respectively (Fig. 4A). pIC-regulated expression was examined for 148 antiviral genes and ISGs (extracted from Refs. 24 and 25 and/or annotated as such in Uniprot). For 47 of these genes, mRNA and/or protein expression were upregulated by pIC at one or more time points (Supplemental Fig. 3). For most (30 genes), upregulation was evident at both the transcript and the protein level. For a smaller portion (15 genes) of induced mRNAs, the corresponding proteins were not detectable or upregulated (Supplemental Fig. 3). Finally, in two cases, only MS detected upregulation. Relatively few mRNAs exhibited robust induction after 2 h, whereas most peaked at 6 h (Fig. 4B, 4C). Most proteins peaked at 18 h (Fig. 4B, 4C). Finally, antiviral proteins were induced significantly more strongly than other upregulated proteins (Fig. 4D). Six of the top 10 most strongly upregulated proteins were encoded by antiviral ISGs (*Ifit1*, *Ifit2*, *Gbp2*, *Oas1a*, *Ifit3*, and *Isg20*; Supplemental Fig. 3C).

Based on fold induction (Supplemental Fig. 3) and biological relevance, 18 antiviral genes (Table I) were selected for Nanostring nCounter (37) analysis. Induction by pIC was confirmed for all 18 mRNAs in both the CD8$^+$ DC line and the primary splenic CD8$^+$ DCs (Fig. 4C). Fold inductions quantified by Nanostring nCounter were markedly stronger than when estimated by microarray analysis (data not shown). Induction was strictly TLR3 dependent because it was abolished in the *Tlr3*$^{-/-}$ CD8$^+$ DC line (Fig. 4E). TLR3 dependence was further confirmed by the finding that polyadenylic-polyuridylic acid, a more TLR3-specific ligand, was as efficient an inducer as pIC (data not shown). Finally, all 18 genes were inducible by both pIC and IFN-α (Fig. 4F).

Identification of primary and secondary TLR3-response genes in CD8$^+$ DCs

Investigations on TLR-induced gene expression have shown that antiviral genes and ISGs can be classified into primary and secondary response genes (23) (Figs. 5A, 6). Primary response genes are induced in the absence of de novo protein synthesis, whereas secondary response ISGs are induced indirectly via production of the primary response gene I-IFN. Primary response genes are typically induced more rapidly by pIC than secondary response ISGs. Furthermore, the latter should be induced more rapidly by IFN-β than pIC. These predictions were validated in the CD8$^+$ DC line for prototypical primary response genes (*Ifit1* and *Isg15*), primary response proinflammatory cytokine genes (*Il12b* and *Il1b*), and secondary response ISGs (*Irf7* and *Mx1*) (Fig. 5B). We therefore categorized ISGs induced in the CD8$^+$ DC line on the basis of two parameters, kinetics of pIC-induced expression (Fig. 5C) and relative induction efficiency by IFN-β versus pIC at an early time point (Fig. 5D). The two approaches correlated remarkably well: pIC-dominant genes exhibited rapid pIC induction, whereas IFN-β–dominant ISGs exhibited delayed pIC induction (Fig. 5E).

To further classify pIC-induced antiviral genes into primary and secondary response genes, we assessed their dependence on de novo protein synthesis using the protein-synthesis inhibitor CHX (Fig. 5F). pIC-dominant genes (including *Ifit1* and *Isg15*) were mainly CHX insensitive, confirming that they are primary response genes. Two pIC-dominant genes (*Rsad2* and *Ifit2*) exhibited partial CHX sensitivity, suggesting that they are primary response genes for which induction is amplified by autocrine IFN-β stimulation. Most IFN-β–dominant ISGs (including *Irf7* and *Mx1*) exhibited CHX-sensitive pIC induction, suggesting that they are secondary response genes. Three genes (*Oasl2*, *Isg20*, and *Ddx58*) were IFN-β dominant but exhibited CHX-insensitive pIC induction, suggesting that they are controlled by nonredundant TLR3 and IFN-β–regulated pathways. For one gene (*Trim30d*), CHX insensitivity could not be established conclusively because it was induced only slightly by pIC after 2 h.

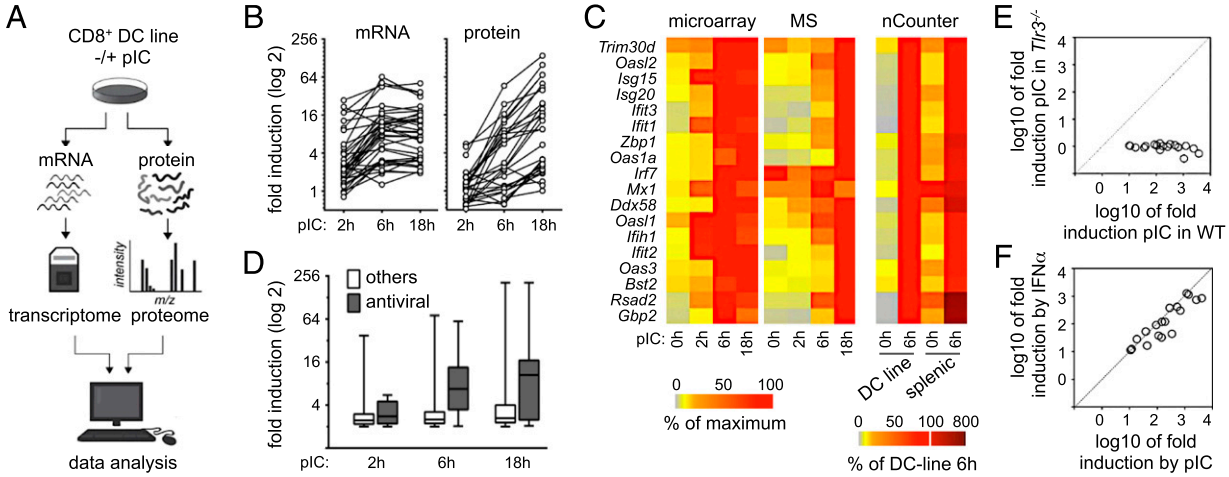

FIGURE 4. Identification of pIC-induced antiviral genes in CD8$^+$ DCs. (**A**) Transcriptomic and proteomic approaches were used to identify antiviral genes induced in the CD8$^+$ DC line. (**B**) Induction kinetics are shown for 47 antiviral genes exhibiting >2-fold increase in mRNA or protein expression in at least one time point. (**C**) Relative mRNA (*left*) and protein (*middle*) expression were determined in the CD8$^+$ DC line stimulated for 0, 2, 6, or 18 h with pIC. Relative mRNA expression was measured by NanoString nCounter (*right*) in the CD8$^+$ DC line and splenic CD8$^+$ DCs stimulated for 0 or 6 h with pIC. Data are expressed relative to maximal mRNA (*left*) or protein (*middle*) expression, or NanoString values for the CD8$^+$ DC line (*right*). Missing MS values were imputed for Irf7. (**D**) pIC-induced proteins with antiviral or other functions induced at 2, 6, and 18 h are shown. (**E**) Fold mRNA induction for 18 antiviral genes was measured by NanoString nCounter in WT and TLR3$^{-/-}$ DC lines stimulated for 6 h with pIC. (**F**) Fold mRNA induction was measured for 18 antiviral genes by NanoString nCounter in the CD8$^+$ DC line stimulated for 6 h with pIC or IFN-α. Results show mean values obtained from three (B–D) or two (E and F) experiments. (E and F) Expression was normalized relative to *Eef1a1*, *Ppia*, *Rpl13a*, *Rplp0*, and *Sdha*.

Discussion

We found that TLR3 engagement can establish a potent cell-autonomous antiviral state in CD8$^+$ DCs. It is likely that a similar antiviral program is triggered by TLR3 engagement in migratory CD103$^+$ DCs, which share with CD8$^+$ DCs the unique property of high TLR3 expression. To dissect the antiviral program induced by TLR3 stimulation in CD8$^+$ DCs, we performed comprehensive mRNA and protein expression profiling experiments. To our knowledge, no such combined transcriptomic/proteomic analyses have been performed in either CD8$^+$ or CD103$^+$ DCs. Such integrated studies have been difficult to perform with primary ex vivo DC subsets. Existing transcriptomic or proteomic analyses of TLR-induced DC activation have mainly exploited mouse GM-CSF–generated BMDCs. However, GM-CSF–generated BMDCs represent monocyte-derived inflammatory DCs, in which TLR3 is lowly expressed, and the recognition of long form of pIC is mediated in large part by cytoplasmic RNA helicase MDA5 (22, 40, 41). The availability of a cell line exhibiting all

Table I. Antiviral ISGs selected for further analysis by the Nanostring nCounter System

MGI Name (Synonym)	Function of Protein	References	Induction by pIC	
			mRNA[a]	Protein[b]
Bst2 (Tetherin)	Blocks release of nascent virions	24, 25	7	17
Ddx58 (Rig-I)	Viral sensing, activation of IRFs	24, 25	21	9
Gbp2	Mainly unknown	24, 25	64	92
Ifih1 (Mda5)	Viral sensing, activation of IRFs	24, 25	16	20
Ifit1	Detects viral 5′-triphosphate RNA, functions within a larger IFIT complex to inhibit viral replication	24, 25, 49	47	144
Ifit2	Associates with 5′-triphosphate RNA indirectly, forms IFN-dependent multiprotein complex with other IFITs	24, 25, 49	22	114
Ifit3	Associates with 5′-triphosphate RNA indirectly, forms IFN-dependent multiprotein complex with other IFITs	24, 25, 49	50	54
Irf7	Transcriptional regulator of IFNs and ISGs	24, 25	14	NA
Isg15	Acts by conjugating target viral (and cellular) proteins in a process termed ISGylation	24, 25	11	17
Isg20	Exonuclease activity	24, 25	18	43
Mx1(MxA)	Formation of highly ordered oligomers	24, 25	9	2
Oas1a	Activates RNaseL to degrade viral genome	24, 25	14	69
Oas3	Activates RNaseL to degrade viral genome	24, 25	8	24
Oasl1	Inhibitor of Irf7 translation, I-IFN negative regulator	50	4	9
Oasl2	Mainly unknown	24, 25	9	17
Rsad2 (Viperin)	Perturbs lipid rafts, promotes TLR7/9 signaling	24, 25	51	39
Trim30d (Trim79α)	Facilitates lysosomal degradation of certain viral polymerases	51	3	2
Zbp1 (DAI)	Recognizes DNA in the cytoplasm, induces the expression of I-IFNs and other genes	52	15	25

[a]Maximum induction determined by microarray analysis.
[b]Maximum induction determined by MS.
IFIT, IFN-induced protein with tetratricopeptide repeats; IRF, IFN regulatory factor; MGI, Mouse Genome Infomatics; NA, not applicable.

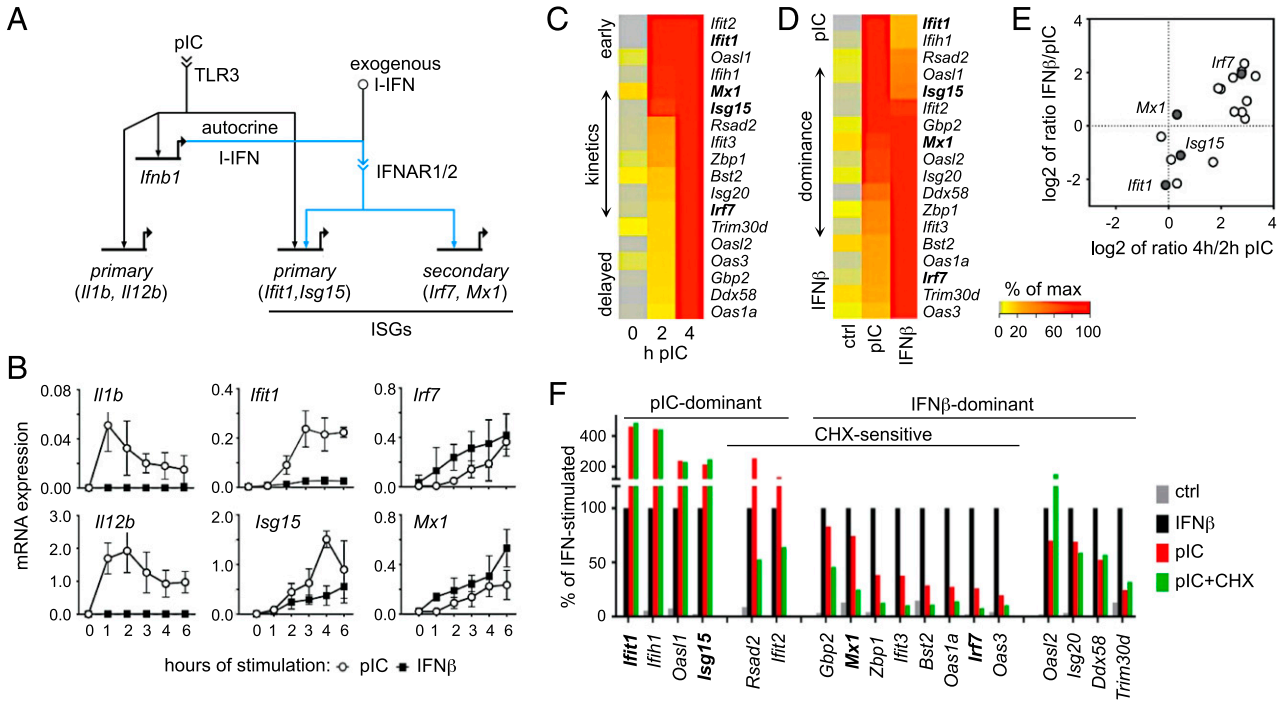

FIGURE 5. Induction of antiviral genes. (**A**) Pathways implicated in gene activation by TLR3 ligands and/or I-IFN. The proinflammatory cytokine genes *Il1b* and *Il12b* are regulated exclusively by pIC (*left*). Certain antiviral genes (*Ifit1* and *Isg15*) are primary TLR3-response genes activated with or without a contribution of I-IFN (*middle*). Others are induced mainly by stimulation with exogenous I-IFN or autocrine TLR3-induced I-IFN production (*right*). (**B**) Induction kinetics of the indicated genes was determined by qPCR in the $CD8^+$ DC line stimulated with pIC and IFN-β. Expression was normalized relative to *Rplp0*. Results are derived from three independent experiments. (**C**–**F**) Expression of 18 antiviral genes was determined by Nanostring nCounter in the $CD8^+$ DC line stimulated with pIC or IFN-β. Genes were ranked according to their relative expression in cells stimulated (C) with pIC for 4 or 2 h and (D) with IFN-β or pIC for 2 h. (E) IFN-β/pIC and 4-h pIC/2-h pIC expression ratios are represented: representative primary and secondary response genes are indicated. (F) mRNA expression is shown as percent of that in the $CD8^+$ DC line stimulated for 2 h with IFN-β. Dependence of pIC-induced expression on de novo protein synthesis was assessed by pretreatment for 0.5 h with CHX. (C–F) Results show mean values obtained from two experiments.

phenotypic and functional features of primary $CD8^+$ DCs thus represented a unique resource.

Establishment of the TLR3-induced antiviral state was abolished in $CD8^+$ DCs lacking the IFNAR1 receptor subunit, implying that it is mediated by autocrine I-IFN stimulation. Although not sufficient to license DCs for priming adaptive immune responses (42, 43), I-IFNs are known to contribute to diverse DC properties, including maturation, cross-presentation, and activation of antitumor and antiviral responses (13, 14, 42, 44–46). I-IFN production is also necessary and sufficient for pIC-induced apoptosis of $CD8^+$ DCs (39). Our results show that the induction of a cell-autonomous antiviral state is a key function of I-IFN production by $CD8^+$ DCs (Fig. 6). III-IFNs cannot replace IFN-β for establishing the TLR3-induced antiviral state because the $CD8^+$ cells lack a functional III-IFNR. This is consistent with the fact that IFN-λR1 expression is restricted to certain cell types, and that most leukocytes do not respond to IFNλ even at high concentrations (47).

Expression profiling studies have shown that I-IFN can induce up to 1000 ISGs, of which 200–500 are typical of many cell types (25). Certain ISGs (estimated at a few dozen) have broad or virus-restricted antiviral effector functions (25, 48). We classified pIC-induced antiviral genes in $CD8^+$ DCs into primary response genes activated directly by TLR3-signaling and secondary response ISGs for which indirect activation via autocrine I-IFN signaling makes a major contribution. Only four ISGs (*Ifit1*, *Ifih1*, *Oasl1*, and *Isg15*) exhibited features expected for primary TLR3-response genes, whereas eight (*Gbp2*, *Mx1*, *Zbp1*, *Ifit3*, *Bts2*, *Oas1a*, *Irf7*, and *Oas3*) exhibited features typical of secondary response genes. The latter are likely to make essential contributions to protection against SeV and VSV in our $CD8^+$ DC system, because the TLR3-induced antiviral effect is strictly dependent on autocrine IFN-β signaling. In contrast, genes for which direct induction by TLR3 signaling is the dominant mechanism are not sufficient for conferring protection against SeV or VSV.

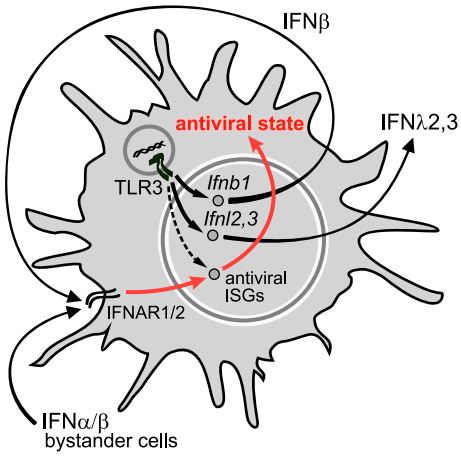

FIGURE 6. Establishment of the antiviral state in $CD8^+$ DCs. TLR3 activation by pIC or virus-derived dsRNA induces the expression of IFN-β, IFN-λ2, IFN-λ3, and antiviral proteins. Although certain antiviral effectors can be induced directly by TLR3 signaling, this is not sufficient to establish the antiviral state because many antiviral genes are induced exclusively or dominantly via autocrine IFN-β stimulation. Exogenous I-IFNs produced by bystander cells, such as pDCs and other cDCs, can replace TLR3 signaling for establishing the antiviral state.

They could, however, collaborate with secondary response ISGs or play key roles in protection against other viruses.

The establishment of a TLR3-induced antiviral state in CD8$^+$ DCs presumably preserves their capacity to prime antiviral T cell responses despite potentially destructive viral loads in secondary lymphoid tissues. The same mechanism could preserve the ability of migratory CD103$^+$ DCs to transport Ags to secondary lymphoid organs through infected tissues and lymphatics containing circulating virus. Furthermore, paracrine stimulation by I-IFN produced by activated CD8$^+$ DCs may contribute to establishing an antiviral state in other cells present in secondary lymphoid tissues, including macrophages, other DC subtypes, T cells, B cells, and nonhematopoietic cells. The mechanism we describe in this article is therefore likely to shield immune responses from the nefarious consequences of viral infection. It could be particularly relevant for viruses detected mainly by TLR3, such as positive ssRNA viruses, which may not trigger I-IFN production by pDCs or other cDC subsets lacking TLR3.

Acknowledgments

We are grateful to members of the Departments of Pathology and Immunology and Microbiology and Molecular Medicine at the University of Geneva, the Department of Biochemistry at the University of Lausanne, and the Department of Biochemistry and Molecular Biology at the University of Debrecen for discussions and technical assistance, particularly Romaine Stalder Monney, Juan Dubrot, Sylvain Lemeille, Christine Lavanchy, Muriel Rosa and Attila Pap. We also acknowledge members of the Genomics Platform at the University of Geneva and Szilard Poliska at the University of Debrecen for help with transcriptomics and bioinformatics.

Disclosures

The authors have no financial conflicts of interest.

References

1. Satpathy, A. T., X. Wu, J. C. Albring, and K. M. Murphy. 2012. Re(de)fining the dendritic cell lineage. *Nat. Immunol.* 13: 1145–1154.
2. Shortman, K., and S. H. Naik. 2007. Steady-state and inflammatory dendritic-cell development. *Nat. Rev. Immunol.* 7: 19–30.
3. Villadangos, J. A., and P. Schnorrer. 2007. Intrinsic and cooperative antigen-presenting functions of dendritic-cell subsets in vivo. *Nat. Rev. Immunol.* 7: 543–555.
4. Mildner, A., and S. Jung. 2014. Development and function of dendritic cell subsets. *Immunity* 40: 642–656.
5. Immunological Genome Consortium. 2012. Deciphering the transcriptional network of the dendritic cell lineage. *Nat. Immunol.* 13: 888–899.
6. den Haan, J. M., S. M. Lehar, and M. J. Bevan. 2000. CD8(+) but not CD8(-) dendritic cells cross-prime cytotoxic T cells in vivo. *J. Exp. Med.* 192: 1685–1696.
7. Shortman, K., and W. R. Heath. 2010. The CD8+ dendritic cell subset. *Immunol. Rev.* 234: 18–31.
8. Kurts, C., B. W. Robinson, and P. A. Knolle. 2010. Cross-priming in health and disease. *Nat. Rev. Immunol.* 10: 403–414.
9. Dudziak, D., A. O. Kamphorst, G. F. Heidkamp, V. R. Buchholz, C. Trumpfheller, S. Yamazaki, C. Cheong, K. Liu, H. W. Lee, C. G. Park, et al. 2007. Differential antigen processing by dendritic cell subsets in vivo. *Science* 315: 107–111.
10. Lauterbach, H., B. Bathke, S. Gilles, C. Traidl-Hoffmann, C. A. Luber, G. Fejer, M. A. Freudenberg, G. M. Davey, D. Vremec, A. Kallies, et al. 2010. Mouse CD8alpha+ DCs and human BDCA3+ DCs are major producers of IFN-lambda in response to poly IC. *J. Exp. Med.* 207: 2703–2717.
11. Schulz, O., S. S. Diebold, M. Chen, T. I. Näslund, M. A. Nolte, L. Alexopoulou, Y. T. Azuma, R. A. Flavell, P. Liljeström, and C. Reis e Sousa. 2005. Toll-like receptor 3 promotes cross-priming to virus-infected cells. *Nature* 433: 887–892.
12. Mashayekhi, M., M. M. Sandau, I. R. Dunay, E. M. Frickel, A. Khan, R. S. Goldszmid, A. Sher, H. L. Ploegh, T. L. Murphy, L. D. Sibley, and K. M. Murphy. 2011. CD8α(+) dendritic cells are the critical source of interleukin-12 that controls acute infection by Toxoplasma gondii tachyzoites. *Immunity* 35: 249–259.
13. Dalod, M., T. Hamilton, R. Salomon, T. P. Salazar-Mather, S. C. Henry, J. D. Hamilton, and C. A. Biron. 2003. Dendritic cell responses to early murine cytomegalovirus infection: subset functional specialization and differential regulation by interferon alpha/beta. *J. Exp. Med.* 197: 885–898.
14. Helft, J., B. Manicassamy, P. Guermonprez, D. Hashimoto, A. Silvin, J. Agudo, B. D. Brown, M. Schmolke, J. C. Miller, M. Leboeuf, et al. 2012. Cross-presenting CD103+ dendritic cells are protected from influenza virus infection. *J. Clin. Invest.* 122: 4037–4047.
15. Desmet, C. J., and K. J. Ishii. 2012. Nucleic acid sensing at the interface between innate and adaptive immunity in vaccination. *Nat. Rev. Immunol.* 12: 479–491.
16. Kawai, T., and S. Akira. 2010. The role of pattern-recognition receptors in innate immunity: update on Toll-like receptors. *Nat. Immunol.* 11: 373–384.
17. Alexopoulou, L., A. C. Holt, R. Medzhitov, and R. A. Flavell. 2001. Recognition of double-stranded RNA and activation of NF-kappaB by Toll-like receptor 3. *Nature* 413: 732–738.
18. Gauzzi, M. C., M. Del Cornò, and S. Gessani. 2010. Dissecting TLR3 signalling in dendritic cells. *Immunobiology* 215: 713–723.
19. Amit, I., M. Garber, N. Chevrier, A. P. Leite, Y. Donner, T. Eisenhaure, M. Guttman, J. K. Grenier, W. Li, O. Zuk, et al. 2009. Unbiased reconstruction of a mammalian transcriptional network mediating pathogen responses. *Science* 326: 257–263.
20. Chevrier, N., P. Mertins, M. N. Artyomov, A. K. Shalek, M. Iannacone, M. F. Ciaccio, I. Gat-Viks, E. Tonti, M. M. DeGrace, K. R. Clauser, et al. 2011. Systematic discovery of TLR signaling components delineates viral-sensing circuits. *Cell* 147: 853–867.
21. Cella, M., M. Salio, Y. Sakakibara, H. Langen, I. Julkunen, and A. Lanzavecchia. 1999. Maturation, activation, and protection of dendritic cells induced by double-stranded RNA. *J. Exp. Med.* 189: 821–829.
22. Jelinek, I., J. N. Leonard, G. E. Price, K. N. Brown, A. Meyer-Manlapat, P. K. Goldsmith, Y. Wang, D. Venzon, S. L. Epstein, and D. M. Segal. 2011. TLR3-specific double-stranded RNA oligonucleotide adjuvants induce dendritic cell cross-presentation, CTL responses, and antiviral protection. *J. Immunol.* 186: 2422–2429.
23. Doyle, S., S. Vaidya, R. O'Connell, H. Dadgostar, P. Dempsey, T. Wu, G. Rao, R. Sun, M. Haberland, R. Modlin, and G. Cheng. 2002. IRF3 mediates a TLR3/TLR4-specific antiviral gene program. *Immunity* 17: 251–263.
24. MacMicking, J. D. 2012. Interferon-inducible effector mechanisms in cell-autonomous immunity. *Nat. Rev. Immunol.* 12: 367–382.
25. Schoggins, J. W., and C. M. Rice. 2011. Interferon-stimulated genes and their antiviral effector functions. *Curr Opin Virol* 1: 519–525.
26. Doyle, S. E., R. O'Connell, S. A. Vaidya, E. K. Chow, K. Yee, and G. Cheng. 2003. Toll-like receptor 3 mediates a more potent antiviral response than Toll-like receptor 4. *J. Immunol.* 170: 3565–3571.
27. Gaajetaan, G. R., T. H. Geelen, G. E. Grauls, C. A. Bruggeman, and F. R. Stassen. 2012. CpG and poly(I:C) stimulation of dendritic cells and fibroblasts limits herpes simplex virus type 1 infection in an IFNβ-dependent and -independent way. *Antiviral Res.* 93: 39–47.
28. Kramer, M., B. M. Schulte, L. W. Toonen, P. M. Barral, P. B. Fisher, K. H. Lanke, J. M. Galama, F. J. van Kuppeveld, and G. J. Adema. 2008. Phagocytosis of picornavirus-infected cells induces an RNA-dependent antiviral state in human dendritic cells. *J. Virol.* 82: 2930–2937.
29. Wang, N., Y. Liang, S. Devaraj, J. Wang, S. M. Lemon, and K. Li. 2009. Toll-like receptor 3 mediates establishment of an antiviral state against hepatitis C virus in hepatoma cells. *J. Virol.* 83: 9824–9834.
30. Kramer, M., B. M. Schulte, D. Eleveld-Trancikova, M. van Hout-Kuijer, L. W. Toonen, J. Tel, I. J. de Vries, F. J. van Kuppeveld, B. J. Jansen, and G. J. Adema. 2010. Cross-talk between human dendritic cell subsets influences expression of RNA sensors and inhibits picornavirus infection. *J. Innate Immun.* 2: 360–370.
31. Hildner, K., B. T. Edelson, W. E. Purtha, M. Diamond, H. Matsushita, M. Kohyama, B. Calderon, B. U. Schraml, E. R. Unanue, M. S. Diamond, et al. 2008. Batf3 deficiency reveals a critical role for CD8alpha+ dendritic cells in cytotoxic T cell immunity. *Science* 322: 1097–1100.
32. Luber, C. A., J. Cox, H. Lauterbach, B. Fancke, M. Selbach, J. Tschopp, S. Akira, M. Wiegand, H. Hochrein, M. O'Keeffe, and M. Mann. 2010. Quantitative proteomics reveals subset-specific viral recognition in dendritic cells. *Immunity* 32: 279–289.
33. Fuertes Marraco, S. A., F. Grosjean, A. Duval, M. Rosa, C. Lavanchy, D. Ashok, S. Haller, L. A. Otten, Q. G. Steiner, P. Descombes, et al. 2012. Novel murine dendritic cell lines: a powerful auxiliary tool for dendritic cell research. *Front. Immunol.* 3: 331.
34. Steiner, Q. G., L. A. Otten, M. J. Hicks, G. Kaya, F. Grosjean, E. Saeuberli, C. Lavanchy, F. Beermann, K. L. McClain, and H. Acha-Orbea. 2008. In vivo transformation of mouse conventional CD8alpha+ dendritic cells leads to progressive multisystem histiocytosis. *Blood* 111: 2073–2082.
35. Tsapogas, P., L. K. Swee, A. Nusser, N. Nuber, M. Kreuzaler, G. Capoferri, H. Rolink, R. Ceredig, and A. Rolink. 2014. In vivo evidence for an instructive role of fms-like tyrosine kinase-3 (FLT3) ligand in hematopoietic development. *Haematologica* 99: 638–646.
36. Mottet-Osman, G., F. Iseni, T. Pelet, M. Wiznerowicz, D. Garcin, and L. Roux. 2007. Suppression of the Sendai virus M protein through a novel short interfering RNA approach inhibits viral particle production but does not affect viral RNA synthesis. *J. Virol.* 81: 2861–2868.
37. Geiss, G. K., R. E. Bumgarner, B. Birditt, T. Dahl, N. Dowidar, D. L. Dunaway, H. P. Fell, S. Ferree, R. D. George, T. Grogan, et al. 2008. Direct multiplexed measurement of gene expression with color-coded probe pairs. *Nat. Biotechnol.* 26: 317–325.
38. Weber, F., V. Wagner, S. B. Rasmussen, R. Hartmann, and S. R. Paludan. 2006. Double-stranded RNA is produced by positive-strand RNA viruses and DNA viruses but not in detectable amounts by negative-strand RNA viruses. *J. Virol.* 80: 5059–5064.
39. Fuertes Marraco, S. A., C. L. Scott, P. Bouillet, A. Ives, S. Masina, D. Vremec, E. S. Jansen, L. A. O'Reilly, P. Schneider, N. Fasel, et al. 2011. Type I interferon

drives dendritic cell apoptosis via multiple BH3-only proteins following activation by PolyIC in vivo. *PLoS ONE* 6: e20189.
40. Xu, Y., Y. Zhan, A. M. Lew, S. H. Naik, and M. H. Kershaw. 2007. Differential development of murine dendritic cells by GM-CSF versus Flt3 ligand has implications for inflammation and trafficking. *J. Immunol.* 179: 7577–7584.
41. Kumar, H., S. Koyama, K. J. Ishii, T. Kawai, and S. Akira. 2008. Cutting edge: cooperation of IPS-1- and TRIF-dependent pathways in poly IC-enhanced antibody production and cytotoxic T cell responses. *J. Immunol.* 180: 683–687.
42. Joffre, O., M. A. Nolte, R. Spörri, and C. Reis e Sousa. 2009. Inflammatory signals in dendritic cell activation and the induction of adaptive immunity. *Immunol. Rev.* 227: 234–247.
43. Spörri, R., and C. Reis e Sousa. 2005. Inflammatory mediators are insufficient for full dendritic cell activation and promote expansion of CD4+ T cell populations lacking helper function. *Nat. Immunol.* 6: 163–170.
44. Swiecki, M., and M. Colonna. 2011. Type I interferons: diversity of sources, production pathways and effects on immune responses. *Curr. Opin. Virol.* 1: 463–475.
45. Honda, K., S. Sakaguchi, C. Nakajima, A. Watanabe, H. Yanai, M. Matsumoto, T. Ohteki, T. Kaisho, A. Takaoka, S. Akira, et al. 2003. Selective contribution of IFN-alpha/beta signaling to the maturation of dendritic cells induced by double-stranded RNA or viral infection. *Proc. Natl. Acad. Sci. USA* 100: 10872–10877.
46. Longhi, M. P., C. Trumpfheller, J. Idoyaga, M. Caskey, I. Matos, C. Kluger, A. M. Salazar, M. Colonna, and R. M. Steinman. 2009. Dendritic cells require a systemic type I interferon response to mature and induce CD4+ Th1 immunity with poly IC as adjuvant. *J. Exp. Med.* 206: 1589–1602.
47. Donnelly, R. P., and S. V. Kotenko. 2010. Interferon-lambda: a new addition to an old family. *J. Interferon Cytokine Res.* 30: 555–564.
48. Schoggins, J. W., S. J. Wilson, M. Panis, M. Y. Murphy, C. T. Jones, P. Bieniasz, and C. M. Rice. 2011. A diverse range of gene products are effectors of the type I interferon antiviral response. *Nature* 472: 481–485.
49. Pichlmair, A., C. Lassnig, C. A. Eberle, M. W. Górna, C. L. Baumann, T. R. Burkard, T. Bürckstümmer, A. Stefanovic, S. Krieger, K. L. Bennett, et al. 2011. IFIT1 is an antiviral protein that recognizes 5′-triphosphate RNA. *Nat. Immunol.* 12: 624–630.
50. Lee, M. S., B. Kim, G. T. Oh, and Y. J. Kim. 2013. OASL1 inhibits translation of the type I interferon-regulating transcription factor IRF7. *Nat. Immunol.* 14: 346–355.
51. Taylor, R. T., K. J. Lubick, S. J. Robertson, J. P. Broughton, M. E. Bloom, W. A. Bresnahan, and S. M. Best. 2011. TRIM79α, an interferon-stimulated gene product, restricts tick-borne encephalitis virus replication by degrading the viral RNA polymerase. *Cell Host Microbe* 10: 185–196.
52. Takaoka, A., Z. Wang, M. K. Choi, H. Yanai, H. Negishi, T. Ban, Y. Lu, M. Miyagishi, T. Kodama, K. Honda, et al. 2007. DAI (DLM-1/ZBP1) is a cytosolic DNA sensor and an activator of innate immune response. *Nature* 448: 501–505.